ARGONNE NATIONAL LABORATORY
9700 South Cass Avenue
Argonne, Illinois 60439

CIM-EARTH: Framework and Case Study

Joshua Elliott, Ian Foster, Kenneth Judd, Elisabeth Moyer, and Todd Munson

Mathematics and Computer Science Division

Preprint ANL/MCS-P1710-1209

February 2010, Revised November 2010

CIM-EARTH: Framework and Case Study*

Joshua Elliott[†] Ian Foster[‡] Kenneth Judd[§]
Elisabeth Moyer[¶] Todd Munson[‖]

December 22, 2010

Abstract

General equilibrium models have been used for decades to obtain insights into the economic implications of policies and decisions. Despite successes, however, these economic models have substantive limitations. Many of these limitations are due to computational and methodological constraints that can be overcome by leveraging recent advances in computer architecture, numerical methods, and economics research. Motivated by these considerations, we are developing a new modeling framework: the Community Integrated Model of Economic and Resource Trajectories for Humankind (CIM-EARTH). In this paper, we describe the key features of the CIM-EARTH framework and initial implementation, detail the model instance we use for studying the impacts of a carbon tax on international trade and the sensitivity of these impacts to assumptions on the rate of change in energy efficiency and labor productivity, and present results on the extent to which carbon leakage limits global reductions in emissions for some policy scenarios.

*We thank Margaret Loudermilk for her help in revising this paper and the referees for their thoughtful comments. This work was supported in part by grants from the MacArthur Foundation and the University of Chicago Energy Initiative and by the Office of Advanced Scientific Computing Research, Office of Science, U.S. Department of Energy, under Contract DE-AC02-06CH11357.

[†]Computation Institute, University of Chicago and Argonne National Laboratory, email: jelliott@ci.uchicago.edu

[‡]Computation Institute, University of Chicago and Argonne National Laboratory, email: foster@anl.gov

[§]Hoover Institution, email: kennethjudd@mac.com

[¶]University of Chicago Department of the Geophysical Sciences, email: moyer@uchicago.edu

[‖]Computation Institute, University of Chicago and Argonne National Laboratory, email: tmunson@mcs.anl.gov

1 Introduction

Computable general equilibrium (CGE) models (Johansen, 1960; Robinson, 1991; Sue Wing, 2004) and their stochastic counterparts, dynamic stochastic general equilibrium models (del Negro and Schorfheide, 2003), form the backbone of policy analysis programs around the world and have been used for decades to obtain insights into the economic implications of policies (Bhattacharyya, 1996; Shoven and Whalley, 1984; de Melo, 1988). Hundreds of such models have been built (Devarajan and Robinson, 2002; Conrad, 2001) and used to explore policy-relevant questions such as the impacts on consumers of new tax policies or increases in fossil energy prices. These models also form a core component when studying the interaction between economic activity and the earth system with an integrated assessment model (Dowlatabadi and Morgan, 1993; Weyant, 2009).

Despite successes, however, these economic models have substantive limitations (Scrieciu, 2007): models may not incorporate the details required to answer questions of interest, cost estimates from different models often differ considerably (Vuuren et al., 2009; Weyant, 1999; de la Chesnaye and Weyant, 2006; Lee, 2006), and little quantification of the uncertainty inherent in these estimates is performed. Many limitations of current models are due to computational and methodological constraints that can be overcome by leveraging advances in computer architecture, numerical methods, and economics research. For example, many contemporary models use simple mathematical formulations, numerical methods, and computer systems that restrict model size and complexity unnecessarily. More modern formulations and solvers and more powerful computer systems offer the potential to solve models several orders of magnitudes larger, while still providing solutions in a reasonable time. Thus, we can in principle create models that incorporate more details of importance to decision makers such as increased industrial, regional, or temporal resolution and capital and commodity vintages (Benhabib and Rustichini, 1991; Cadiou et al., 2003; Salo and Tahvonen, 2003). For example, understanding the distributional impacts of carbon emission policies (Fullerton, 2009; Fullerton and Rogers, 1993) requires overlapping generations for each income group (Auerbach and Kotlikoff, 1987). Having these models, we can then study the interactions between policies that vary by region and characterize important aspects of uncertainty such as the sensitivity of model outputs to baseline assumptions.

Motivated by these considerations, we are developing a new modeling framework: the Community Integrated Model of Economic and Resource Trajectories for Humankind (CIM-EARTH). Our goal is to facilitate and encourage the creation, execution, and testing of new economic models with significantly greater fidelity and sophistication than is the norm today. We envision the framework as combining (a) high-level programming that permits the convenient formulation of a wide range of models, (b) a flexible implementation that permits the efficient solution of these models using advanced numerical methods and high-performance computer systems, and (c) a suite of tools for parameter estimation and model evaluation.

We seek not only to provide access to better economic formulations and numerical methods but also to encourage the development and use of open models. Transparent policy studies require that software and data be *accessible* and *understandable*. Thus, we distribute our framework under an open-source license that permits others to read the software, modify it, and redistribute the modifications. Equally important, we structure the code in a way that makes its meaning readily apparent. In addition, we design our software to be *modifiable* and *extensible*, so as to facilitate the reuse of methodologies and tools; a model generated by one researcher can be tested by others with different data, compared to other models, and extended in new directions. In this way, the barriers to entry for newcomers are greatly reduced, increasing the diversity and quality of the ideas explored.

In this paper, we describe the key features of the CIM-EARTH framework (Section 2), detail the particular model instance we use for studying the impacts of a carbon tax on international trade and the sensitivity of these impacts to the assumptions used to construct a baseline scenario (Section 3), and present results on the extent to which carbon leakage limits global reductions in emissions for a handful of policy scenarios (Section 4). We conclude in Section 5.

The focus of this paper is the tools and techniques employed, rather than a detailed policy analysis. In particular, Section 3.2 develops an ensemble of baseline scenarios for sensitivity studies using the energy efficiency and labor productivity parameters that are highly relevant when analyzing emission abatement policies, Section 4.1 describes our method for measuring embedded carbon in goods and services for use in estimating the carbon content of international trade flows, Section 4.2 introduces a matrix method for displaying international carbon flows in order to visualize the impacts of climate policies, and Section 4.3 provides results over our ensemble of baseline scenarios. These tools and techniques can be adapted for more detailed studies of carbon leakage and for other policy studies. Scalar versions of the model used in the case study are available from `www.cim-earth.org`.

2 CIM-EARTH Framework

To develop an accessible, understandable, modifiable, and extensible framework, our overall architecture uses a modular design; proven numerical libraries such as PATH (Dirkse and Ferris, 1995; Ferris and Munson, 1999, 2001), TAO (Benson et al., 2010), and PETSc (Balay et al., 1997); and a high-level specification language. We discuss here those parts of the CIM-EARTH framework that are concerned with specifying and solving CGE models.

CGE models determine prices and quantities for commodities such that supply equals demand (Ballard et al., 1985; Ginsburgh and Keyzer, 1997; Scarf and Shoven, 1984). Such models may feature the following:

- Many *industries* that each hire labor, rent capital, and buy inputs to produce an output. Each industry chooses a feasible production schedule to maximize its profit.
- Many *consumers* that choose what to buy and how much to work subject to the constraint that expenditures cannot exceed income. Each consumer chooses a feasible consumption schedule to maximize his utility function.
- Many *markets* where industries and consumers trade and where wage rates and commodities prices are set to clear the markets. In particular, if the price of a commodity is positive, then supply must equal demand.

Model instances are specified by defining the type of model (deterministic or stochastic, myopic or forward looking); the size of the model (number of regions, industries, consumers, and time periods); the details for the industries and consumers (production and utility functions and their nested structure), their parametrization (elasticities of substitution) and calibration data (expenditures and tax data for the base year); dynamic trajectories (land and labor endowments, energy efficiency, and capital accumulation); and any coupling with other system components.

The initial version of the CIM-EARTH framework has been implemented in the AMPL modeling language (Fourer et al., 2003). This language is convenient for expressing large optimization and complementarity problems using sets and algebraic constraints, provides access to a variety of commercial and academic numerical methods, and automatically computes the derivative information required by these methods when calculating a solution. We are currently developing a next-generation system that uses a domain-specific language to simplify model specification and can utilize parallel computers when solving large models.

Figure 1: **Basic nesting for production function.**

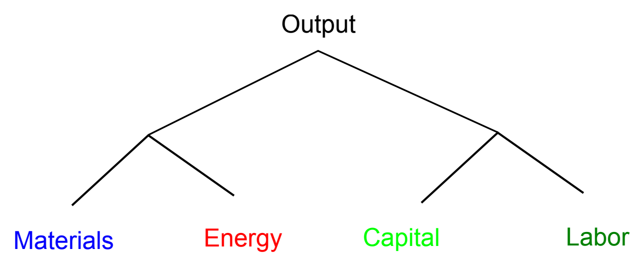

The primary challenge in developing such models is estimating the production and utility functions that characterize the physical and economic processes constraining the supply and demand decisions of industries and consumers. For our CGE models, we use nested constant elasticity of substitution (CES) production and utility functions in calibrated share form (Boehringer et al., 2003),

$$\mathbf{y} = \left(\sum_i \theta_i \left(\gamma_i \mathbf{x}_i \right)^{\frac{\sigma-1}{\sigma}} \right)^{\frac{\sigma}{\sigma-1}},$$

where $\mathbf{y}$ is the ratio between the output of the industry to a base-year value, $\mathbf{x}_i$ are the ratios of the inputs to their base-year values, γ_i are efficiency parameters that determine how effectively these factors can be used, θ_i are the share parameters with $\theta_i > 0$ and $\sum_i \theta_i = 1$, and σ controls the degree to which the inputs can be substituted for one another. The special cases of Leontief (σ=0) and Cobb-Douglas (σ=1) functions are supported by our framework.

The nesting structure is depicted graphically by a tree, with each node representing a production function with its own elasticity of substitution that aggregates the inputs from below into a bundle. The root node represents the total output from the production process. Figure 1 shows a simple case. In the CIM-EARTH framework, we add intermediate variables for the internal nodes, encode the individual functions by specifying the inputs and output, and reconstruct the tree from this information. Since the nesting structure is typically the same for each industry independent of the region in which it resides, we provide facilities to convey this information and reduce the amount of required coding.

Tables are used to convey the parametrization and calibration data. These data include expenditures on inputs and tax information. The share parameters are automatically computed given the nesting structure of the production functions and the expenditure data for the base year. Also included is support for ad valorem and excise taxes, import and export duties, and endogenous tax rates such as those encountered in cap-and-trade policies.

Once the model structure and data are provided, we enter a preprocessing phase to check consistency and make any necessary modifications. Consistency checks include testing the nesting structure to ensure it is a tree. Modifications are made to the tree structure, for example, to eliminate inputs that have zero expenditures or minuscule shares. The modifications are applied iteratively so that if all the branches of a particular node are eliminated, that node is also eliminated. Such modifications are necessary to ensure that the nesting structure matches the expenditure data.

After preprocessing is complete, we have a set of constrained optimization problems for the industries and consumers and market clearing conditions. Because the optimization problems solved by the industries and consumers are convex in their own variables and satisfy a constraint qualification, we can replace each with an equivalent complementarity problem obtained from the first-order optimality conditions by adding Lagrange multipliers on the constraints. These optimality conditions in combination with the market clearing conditions form a square complementarity problem.

The simplest dynamic CGE models are *myopic*, meaning that industries and consumers look only at their current state and do not consider the future. In this case, after the preprocessing step, we loop over time and solve a complementarity problem for each time step with fixed trajectories for land and labor endowments, efficiency parameters, and emission factors. The capital stocks are dynamically updated at the end of each time period based on depreciation and investment. Summary reports are written to user-defined files once the complementarity problem for each time step is solved.

The complementarity problem solved at each time step is automatically generated by the framework and is emitted in a scalar form so that it can be inspected. The complementarity problem is solved by applying a generalized Newton method such as PATH (Dirkse and Ferris, 1995; Ferris and Munson, 1999, 2001). PATH is a sophisticated implementation of a Josephy-Newton method that solves a linear complementarity problem at each iteration using a variant of Lemke's method to obtain a direction and then searches along this direction to obtain sufficient decrease for the merit function.

3 Model Instance

We next provide a detailed discussion of the model instance implemented in the CIM-EARTH framework used for studying the impacts of a carbon tax on international trade and the sensitivity of these impacts to the assumptions used to construct a baseline scenario. In particular, we specify the structure of the production functions and the data used to calibrate them in Section 3.1 and the exogenous trajectories for important economic drivers that define an ensemble baseline scenarios in Section 3.2.

3.1 Structure

Table 1 shows the regions, industries, and factors in the model instance used for our study. The regions are labeled with the aggregation used for reporting purposes. For each industry we indicate the structure of the production functions: (A) agriculture, (E) extraction of fossil fuels, (M) manufacturing, (N) electricity generation, (P) petroleum refining, and (S) service industries. This industry aggregation was chosen to contain more detailed resolution in the energy-intensive industries and in the industries that provide transport services to importers for moving commodities around the world, since these industries would be most affected by a carbon tax or cap-and-trade program.

The production functions in each region have the nested structure summarized in Figure 2 and are loosely based on those used in the EPPA model (Babiker et al., 2001). As before, each node represents a CES function aggregating the production factors below it. The structure of the production functions for the importers of each commodity in each region is also provided. In addition, there is a capital goods industry in each region that aggregates materials using a single Leontief production function. The capital goods industries do not demand fossil fuels, refined petroleum, electricity, or production factors. These capital goods produced are demanded only by consumers in their role as investors. All these industries are subject to ad valorem and excise taxes. We use elasticities of substitution taken from the CGE literature for the industries and consumers (Balistreri et al., 2003; Liu et al., 2004; Webster et al., 2008; Sokolov et al., 2009) and the GTAP database for the base-year revenues, expenditures, and tax data. In particular, the share parameters are calibrated with the GTAP version 7 database of global expenditure values with a 2004 base year (Gopalakrishnan and Walmsley, 2008).

Trade among regions is handled through importers of each commodity in each region. Importers are modeled like other industries using the nested

Table 1: **Regions, industries, and factors for the CGE model used for this study.**

Regions	Industries	Factors
United States (USA)	Agriculture and Forestry (A)	Capital
Western Europe (EUR)	Coal Extraction (E)	Labor
Rest of Europe (EUR)	Gas Extraction (E)	Land
Russia, Georgia, and Asiastan (RUS)	Oil Extraction (E)	Nat. Resources
Japan (JAZ)	Cement (M)	
Oceania (JAZ)	Chemicals (M)	
Canada (CAN)	Nonferrous Metals (M)	
China, Mongolia, and Koreas (CHK)	Steel and Iron (M)	
Brazil (LAM)	Other Manufacturing (M)	
Mexico (LAM)	Electricity (N)	
Rest of Latin America (LAM)	Petroleum Refining (P)	
Middle East and North Africa (ROW)	Air Transport (S)	
Rest of Africa (ROW)	Land Transport (S)	
India (ROW)	Sea Transport (S)	
Rest of South Asia (ROW)	Government Services (S)	
Rest of Southeast Asia (ROW)	Other Services (S)	

Note: The regions are labeled with the aggregation used for reporting the results obtained. The industries are labeled by their production function structure: (A) agriculture, (E) extraction of fossil fuels, (M) manufacturing, (N) electricity generation, (P) petroleum refining, and (S) service industries.

CES production function shown in Figure 2. Table 2 shows the elasticities of substitution between domestic and imported commodities and the Armington international trade elasticities used for this study. We use a Leontief production function to aggregate between the imported commodity and the relevant total transport margin, so that the amount of transport demanded scales with the amount of the commodity imported. We use three types of transportation: land transportation, including freight by trucks and pipelines; air transportation; and sea transportation. Since importers do not care about the origination of these transport services, we model international transportation of each type as a homogeneous commodity with one global price. The model instance has separate homogeneous transportation service industries for air, land, and sea transportation. Each aggregates a single type of domestic transportation service from all regions into a single commodity using a Cobb-Douglas production function. These homogeneous transportation services are used only for international trade; domestic transportation services are included in the materials nest of the other production functions.

This model does not contain a government consumer; it contains only a government services industry, which include defense, social security, health care, and education. Industries and consumers demand these government ser-

Figure 2: **Structure of the production functions for the model instance used for this study.**

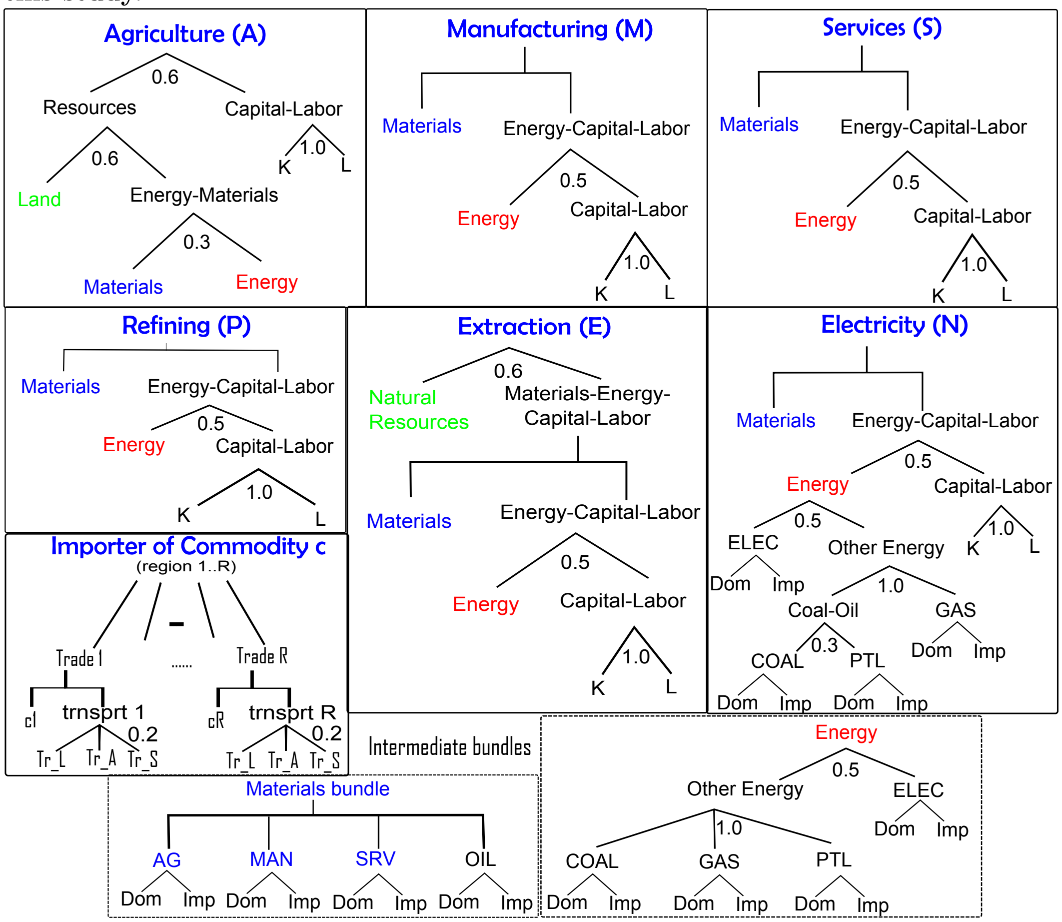

Note: Each node represents a production function. Nodes with vertical line inputs use Leontief functions; the other nodes are labeled with their elasticities of substitution. Table 2 shows the elasticities of substitution between domestic and imported commodities and the Armington international trade elasticities.

vices. The government services industry is treated like any other industry and is subject to ad valorem and excise taxes. All taxes collected by a region are returned to consumers in that region.

Capital is specific to each region in the model instance. Within each region, we use a perfectly fluid capital model with a 4% yearly depreciation rate. To spur investment in capital, we use the standard practice in myopic CGE models in which investment contributes to consumer utility with the

Table 2: **Elasticity of substitution parameters between domestic and imported commodities and the Armington international trade elasticities by industry for the CGE model used for this study.**

	Elasticity of Substitution	
Industry	Domestic/Import	Armington
Agriculture and Forestry (A)	2.7	5.6
Coal Extraction (E)	3.0	6.1
Gas Extraction (E)	17.2	34.4
Oil Extraction (E)	5.2	10.4
Cement (M)	2.9	5.8
Chemicals (M)	3.3	6.6
Nonferrous Metals (M)	4.2	8.4
Steel and Iron (M)	3.0	5.9
Other Manufacturing (M)	3.4	7.2
Electricity (N)	2.8	5.6
Petroleum Refining (P)	2.1	4.2
Air Transport (S)	1.9	3.8
Land Transport (S)	1.9	3.8
Sea Transport (S)	1.9	3.8
Government Services (S)	1.9	3.8
Other Services (S)	1.9	3.8

Note: The industries are labeled by their production function structure: (A) agriculture, (E) extraction of fossil fuels, (M) manufacturing, (N) electricity generation, (P) petroleum refining, and (S) service industries.

investment amount calibrated to historical data. In particular, the investment commodity the consumer buys is the output from the capital goods industry. Investment enters the consumer utility function in a Cobb-Douglas nest with the government services and consumption bundles, implying that fixed shares of consumer income in each year is used for government services, investment, and consumption. The change in the capital endowment in the next period relative to the amount in the base year is obtained from the dynamic equation

$$\mathbf{y}_{K,t+1} = (1-\delta)\mathbf{y}_{K,t} + \frac{\bar{x}_{I,0}}{\bar{y}_{K,0}}\mathbf{x}_{I,t},$$

where $\mathbf{y}_{K,t}$ is the change in capital endowment ($\mathbf{y}_{K,0}$=1), $\mathbf{x}_{I,t}$ is the change in investment, and δ is the capital depreciation rate. The ratio of the base-year investment quantity $\bar{x}_{I,0}$ to the base-year capital stock $\bar{y}_{K,0}$ is available from the GTAP database.

3.2 Ensemble of Baseline Scenarios

We construct an ensemble of trajectories for important economic drivers such as labor productivity and energy efficiency by extrapolation from historical data that are input into the model instance. By running the model instance for each set of forecasts without making any policy changes, we obtain an ensemble of baseline scenarios that can be compared to existing baseline scenarios from the literature. Moreover, by exploring policy scenarios over a range of baseline scenarios, we can determine the sensitivity of a policy to the assumptions used to generate the baseline scenario.

Our approach differs from much of the carbon leakage literature that typically starts from a reference baseline scenario, chooses a single set of trajectories to replicate it, and then determines the change in outcome for a variety of policy scenarios, often without discussion of the scientific underpinnings of the baseline scenario or how it has been integrated into the model. While the trajectory of CO_2 emissions, for example, may match the EIA forecast, the parameters tuned to achieve this result and thus the assumptions made are not described. This lack of documentation makes it difficult to compare results to the literature, since the results are reported relative to a single hypothetical baseline scenario for which the assumptions are not defined.

We now detail the construction of our ensemble of baseline scenarios, which are parametrized by national aggregate energy efficiency and labor productivity parameters. The space is reduced to two dimensions by assuming perfect correlations for energy efficiency and labor productivity across regions. We then compare the results from our baseline scenarios to forecasts of emissions from the literature.

3.2.1 Energy Efficiency

We incorporate an energy efficiency parameter into each industry production function to model the efficiency by which their input energy is used. The inverse of regional industrial energy intensity is used as a proxy for the energy efficiency of industry. Historical industry gross domestic product is obtained from the UN database of national accounts, and historical industry energy use is obtained from the IEA World Energy Balance database. These data are used to calculate the yearly rate of change in industrial energy intensity. Rates for all regions in our model instance are available from 1972 to 2007. We truncate the data set to eliminate the two largest positive and negative rates of change to eliminate strong variations from one-time political events or economic crashes.

The median baseline scenario forecasts a constant rate of change in energy intensity after 2008 equal to a weighted geometric mean of the historical rates. Minimum and maximum values on the forecast rate of change in energy intensity for the other baseline scenarios are obtained using the standard deviation of the historical rate data with a skewness factor. The skewness factor is related to the slope of a linear regression model of the historical rate data. For regions with a negative slope in the linear regression model, the rate of change in energy intensity for the forecast years is skewed lower. Positive slopes are treated similarly. In particular, we use

$$\begin{aligned} \min &= \mu - \tfrac{\sigma}{4} + 5\beta \\ \max &= \mu + \tfrac{\sigma}{4} + 5\beta \end{aligned} \tag{1}$$

where μ is the geometric mean of the historical data, σ is the standard deviation, and β is the slope of the linear regression model. The only exception is for the "Rest of Europe" region, where rapid increases in energy efficiency in recent years from technological improvements and economic shifts spurred by membership in the European Union would forecast an energy efficiency level surpassing the gross energy efficiency levels forecast for the more developed parts of Europe, the United States, and Japan by 2030–2040. Since these efficiency levels seem highly unlikely, the skewness factor is set to zero for this region. The minimum, median, and maximum values for the forecast rate of change in energy intensity for each region is found in Table 3. Intermediate values are obtained by linear interpolation. Negative values for the rate of change in energy intensity imply increased energy efficiency.

3.2.2 Population Growth and Labor Productivity

The other economic drivers we consider are population growth and labor productivity, which are combined to estimate the labor endowment in each region. We use gross population data from 1950 to 2008 with forecasts to 2050 from the 2008 United Nations population database (United Nations, 2008) and historical economic activity rates from 1980 to 2006 from the International Labor Organization (International Labor Organization, 2010) with projections to 2020 to determine the economically active segment of the population.

Labor productivity is chosen to match forecasts extrapolated from historical trends using data from the International Labor Organization Database of Key Indicators of the Labor Market (International Labor Organization, 2009). This database contains data for most countries spanning 1980 to 2005. For simplicity, we currently base labor productivity on the index of gross domestic product per person employed, even though productivity indices are

Table 3: **Maximum, median, and minimum values for the average percent rate of change in energy intensity and labor productivity.**

	Energy Intensity			Labor Productivity		
Region	max	median	min	max	median	min
United States	-1.65	-2.51	-3.17	1.93	1.76	1.59
Western Europe	-1.74	-2.09	-2.46	1.58	1.45	1.31
Rest of Europe	-1.39	-2.41	-3.43	3.83	3.26	2.70
Russia, Georgia, and Asiastan	-1.08	-1.88	-3.71	2.64	1.63	0.62
Japan	-0.97	-1.80	-2.19	1.94	1.69	1.45
Oceania	0.28	-0.35	-0.98	1.82	1.54	1.25
Canada	-0.75	-1.31	-2.10	1.57	1.33	1.08
China, Mongolia, and Koreas	-1.93	-2.54	-3.63	7.62	6.89	6.16
Brazil	1.02	0.67	0.32	1.27	0.27	0.09
Mexico	-1.48	-2.07	-3.38	1.34	0.38	0.25
Rest of Latin America	-0.17	-0.44	-1.68	1.28	0.78	0.27
Mid East and North Africa	0.83	0.07	-1.36	1.75	1.32	0.88
Rest of Africa	-0.77	-1.09	-1.98	1.24	0.76	0.29
India	-1.53	-1.92	-2.99	4.45	4.01	3.56
Rest of South Asia	0.09	-1.03	-1.78	2.78	2.50	2.21
Rest of Southeast Asia	0.30	-0.74	-1.73	4.31	3.82	3.33

Note: The median value is the linearly weighted geometric mean and the min and max values are defined in (1).

available at sectoral resolution covering agriculture, forestry and fishing, manufacturing, trade, and transportation and communication for many countries. Forecasts of the rate of change in labor productivity are constructed in a manner similar to the energy efficiency parameter. In particular, our median baseline scenario assumes a constant rate of change in labor productivity equal to a weighted geometric mean of the historical rates. The skewness parameter is set to zero for all regions except Mexico and Brazil when determining the minimum and maximum values because it either has a negligible impact or produces unrealistic maximum values. For Mexico and Brazil, the skewness parameter is set to the slope of the linear regression model to prevent the minimum rate of change in the labor productivity parameter from becoming negative. While the rate of change in labor productivity could be negative for some regions over the next 25 years in some time periods, a sustained negative rate of change in labor productivity is not realistic. The minimum, median, and maximum values for the forecast labor productivity intensity for each region are found in Table 3.

Figure 3: **Percent rate of change in global CO_2 emissions.**

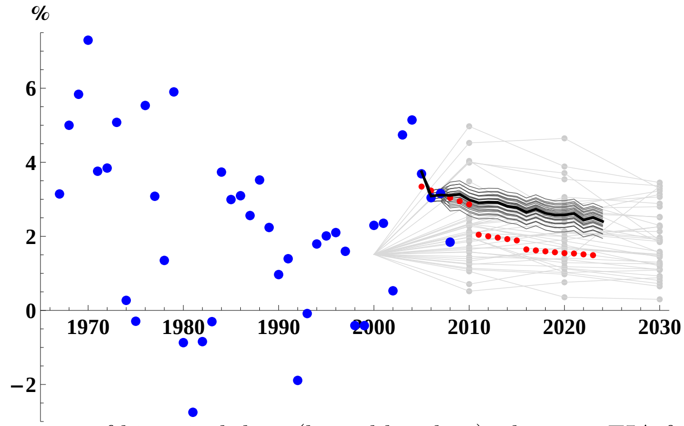

Note: The comparison of historical data (large blue dots), the 2005 EIA forecast (small red dots), SRES scenarios (light gray connected dots), and our ensemble of baseline scenarios (dark solid lines) is plotted as yearly rates of change.

Figure 4: **Global gross CO_2 emissions.**

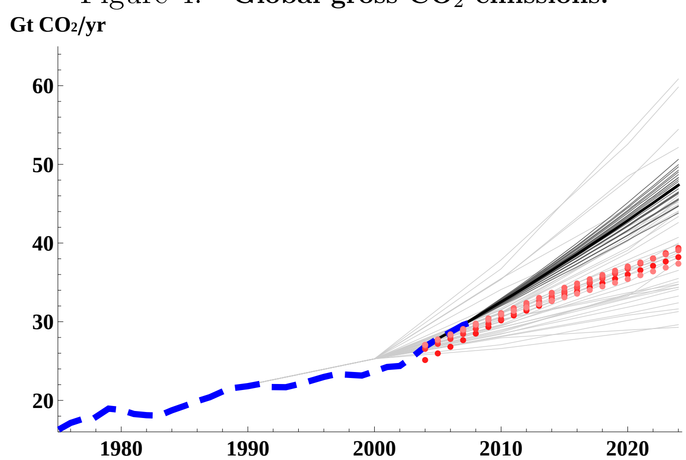

Note: The comparison of historical data (dashed blue line), 2005–2009 EIA forecasts (small red dots), SRES scenarios (light gray solid lines), and our ensemble of baseline scenarios (dark solid lines) is plotted as gross annual emissions.

3.2.3 Comparison to Emission Forecasts

By assuming perfect correlation among regions, we generate an ensemble of baseline scenarios containing 25 members by taking the cross product of five energy intensity and five labor productivity levels. In one scenario, for example, each region uses the minimum value for their energy intensity parameter and the maximum value for their labor productivity parameter. Figures 3–8 compare the emissions generated by our model instance for each element of

Figure 5: **Percent rate of change in USA CO_2 emissions.**

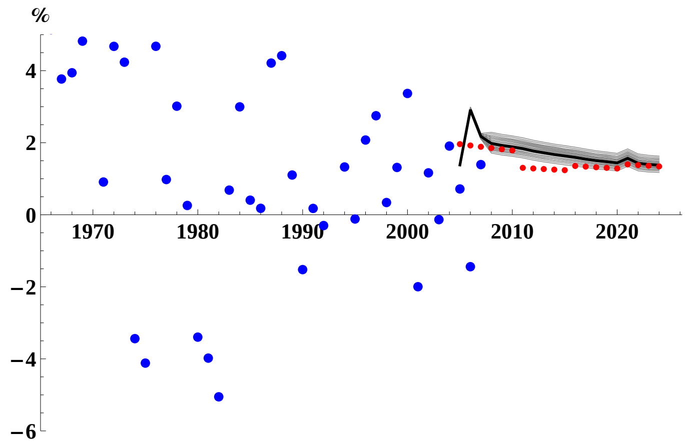

Note: The comparison of historical data (large blue dots), the 2005 EIA forecast (small red dots), and our ensemble of baseline scenarios (dark solid lines) is plotted as yearly rates of change.

Figure 6: **USA gross CO_2 emissions.**

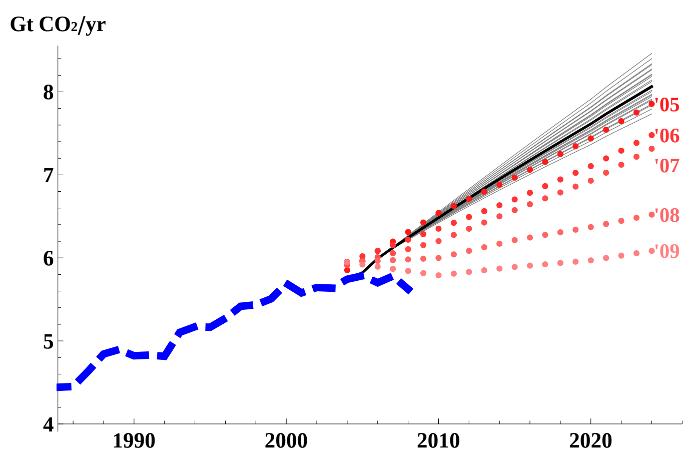

Note: The comparison of historical data (dashed blue line), the 2005–2009 EIA forecasts (small red dots), and our ensemble of baseline scenarios (dark solid lines) is plotted as gross annual emissions. The EIA forecasts are labeled by the year they were released to highlight the direction of the significant changes over the last 5 years.

the baseline ensemble to historical CDIAC data (Boden et al., 2009), 2005–2009 EIA reference case forecasts (United States Energy Information Agency, 2009), and 40 SRES scenarios from the IPCC AR4 (Nakicenovic et al., 2000). The unit for the reported gross emissions is billions of tonnes (Gt) CO_2.

Our model is calibrated from data up to and including 2005 and we have made no effort to account for the recent global recession. In particular,

Figure 7: **Percent rate of change in CHK CO_2 emissions.**

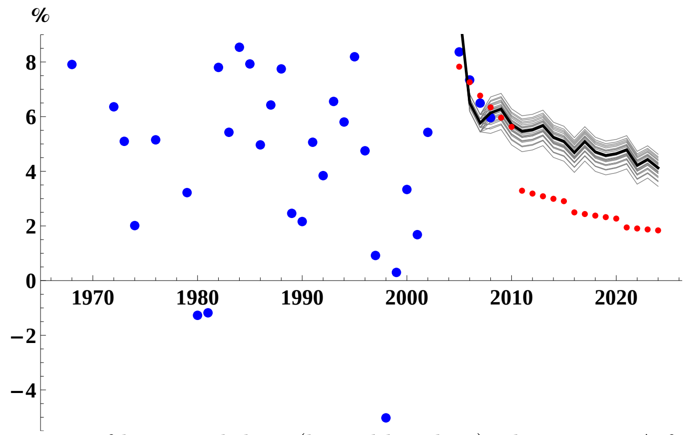

Note: The comparison of historical data (large blue dots), the 2005 EIA forecast (small red dots), and our ensemble of baseline scenarios (dark solid lines) is plotted as yearly rates of change.

Figure 8: **CHK gross CO_2 emissions.**

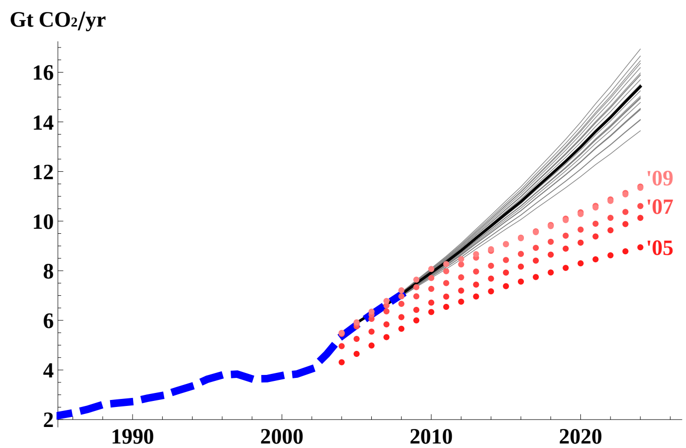

Note: The comparison of historical data (dashed blue line), the 2005–2009 EIA forecasts (small red dots), and our ensemble of baseline scenarios (dark solid lines) is plotted as gross annual emissions. The EIA forecasts are labeled by the year they were released to highlight the direction of the significant changes over the last 5 years.

the trajectory for the USA is similar to the 2005 EIA baseline both in the yearly rate of change (Figure 5) and in gross emissions (Figure 6). The EIA has adjusted their baseline USA forecasts substantially over the last 5 years. In particular, the slope of the EIA forecasts has been significantly modified. While we appreciate that the global recession has produced several years of flat or reduced emissions, we see no structural changes to the economy that would cause the rate of emissions growth to stay low once economic growth returns to previous levels, and so have not built this effect into the baseline ensemble.

The difference between the rate of change and gross emissions trajectories for the global aggregate in our baseline ensemble and the baseline forecasts produced by the EIA are due almost entirely to the divergence between forecasts for CHK beyond 2010. Since our parameters are rooted in extrapolation from the historical record, our trajectories miss the dramatic slowing in emissions for CHK forecast by the EIA. Our baseline trends show a decline in the yearly rate of change in emissions for CHK after 2011 which is consistent with the EIA forecasts. The significant drop in the rate of change in CHK emissions in 2010, however, is not represented. In particular, the rate of change in emissions for CHK in the EIA forecasts drops from 6% for 2009 to just more than 3% for 2010 and continues to decline beyond 2010.

4 Case Study

In our case study, we examine the impacts of a carbon tax on international trade, the extent to which carbon leakage limits global reductions in emissions, the impact of border tax adjustments on reducing carbon leakage, and the sensitivity of these impacts to the assumptions used to generate the baseline scenario. To determine the extent of the carbon leakage for a particular policy, we must first measure the emissions embedded in the traded commodities. Our approach to carbon accounting is detailed in Section 4.1. We report results from four policy scenarios in Section 4.2 using a matrix to visualize international emission flows and then evaluate the dependence of the emission forecasts to the underlying baseline scenario assumptions in Section 4.3.

4.1 Carbon Accounting

We measure the embedded emissions in each commodity by assuming conservation of emissions. In particular, the emissions content of the output for an industry is the sum of the emissions content of the constituent inputs and the emissions generated during the production process from burning fossil fuels. Alternative methods for determining emissions content can be found in Davis and Caldeira (2010), for example.

Specifically, conservation of emissions is stated as

$$E_{j,t}y_{j,t} = \sum_i \left(E_{i,t} + e_i^j\right) x_{i,t}^j \tag{2}$$

where $E_{j,t}$ is the emissions content per unit of commodity j at time t, $y_{j,t}$ is the quantity of commodity j output by the industry, e_i^j is an emissions factor that determines the emissions generated per unit from input commodity i during the production process, and $x_{i,t}^{j}$ is the quantity of input commodity i used in the production of commodity j at time t. The emissions directly generated by industry j at time t is the summation $\sum_i e_i^j x_{i,t}^j$, while global emissions is $\sum_j \sum_i e_i^j x_{i,t}^j$, which equals the sum of the embedded emissions in all the commodities consumed when the markets clear.

The emissions factors are positive when the input is a fossil fuel that is burned and zero for all other inputs. The emission factors are industry specific to account for regional and industrial differentiation in the types of input commodities and their emission rates. For example, the steel industry uses a large amount of coking coal with a high carbon content, while the electricity generated by coal-fired power plants typically comes from lignite with a low carbon content. Further, some industries use fossil inputs in the generation of their outputs but do not burn them and hence have no new emissions generated from them. In particular, the chemicals and plastics industries use natural gas in their production processes, but do not burn the natural gas.

For a simple example, assume we have four commodities, coal, electricity, steel, and automobiles, where coal is burned to generate electricity, electricity is used to produce steel and automobiles, steel is used to produce automobiles, and consumers demand the automobiles. Given 10 units of each commodity, we would then solve the system of equations

$$\begin{aligned} 10E_{coal} &= 0 \\ 10E_{elec} &= 10\left(E_{coal} + e_{coal}\right) \\ 10E_{steel} &= 7E_{elec} \\ 10E_{auto} &= 3E_{elec} + 10E_{steel}, \end{aligned}$$

where the emissions factor for coal, e_{coal}, is known and we assume that the production of coal does not generate any emissions. All emissions in this example are generated from burning coal to produce electricity and total $10e_{coal}$ emission units. The solution to the system of equation is

$$\begin{aligned} E_{coal} &= 0 \\ E_{elec} &= e_{coal} \\ E_{steel} &= 0.7e_{coal} \\ E_{auto} &= e_{coal}. \end{aligned}$$

Since consumers demand all the automobiles produced, the emissions content of the automobiles demanded, $10E_{auto}$, equals the total emissions generated.

CGE models do not typically determine the actual quantities supplied and demanded, but rather calculate the change in quantity relative to a base year. Therefore, we rewrite (2) as

$$E_{j,t}\bar{y}_j\mathbf{y}_{j,t} = \sum_i (E_{i,t} + e_i^j)\bar{x}_i^j\mathbf{x}_{i,t}^j \,,$$

where $\bar{y}_j$ is the base-year volume of commodity j output by the industry and $\mathbf{y}_{j,t}$ is the change in output relative to the base year at time t with $y_{j,t} = \bar{y}_j\mathbf{y}_{j,t}$, and $\bar{x}_i^j$ is the base-year volume of commodity i input for the production of commodity j and $\mathbf{x}_{i,t}^j$ is the change in demand relative to the base year for those inputs at time t with $x_{j,t} = \bar{x}_j\mathbf{x}_{j,t}$. The emissions generated by the producers from each input in the base year, $\bar{f}_i^j = e_i^j\bar{x}_i^j$, is obtained from the energy volume information in the GTAP-E database (Burniaux and Truong, 2002).

Moreover, the base-year quantities in the emissions expression, $E_i\bar{x}_i^j$, are generally unavailable. Hence, we compute the total emissions for the industry rather than compute the emissions content per commodity unit. In particular, we make the substitution

$$F_{j,t} = E_{j,t}\bar{y}_j$$

to obtain the equivalent system

$$F_{j,t}\mathbf{y}_{j,t} = \sum_i \left(F_{i,t}\frac{\bar{x}_i^j}{\bar{y}_i} + \bar{f}_i^j \right) \mathbf{x}_{i,t}^j \,.$$

In those cases where we know the base-year volume data, we directly compute the ratio of $\bar{x}_i^j$ to $\bar{y}_i$. In all other cases, we compute the ratio from available expenditure data,

$$\frac{\bar{x}_i^j}{\bar{y}_i} = \frac{\bar{p}_i\bar{x}_i^j}{\bar{p}_i\bar{y}_i} = \frac{\bar{e}_i^j}{\bar{r}_i} \equiv \Phi_i^j \,,$$

where $\bar{p}_i$ is the base-year price of commodity i. The expenditure and revenue data for each industry, $\bar{e}_i^j$ and $\bar{r}_i$, respectively, are known from the base-year calibration data. In particular, Φ_i^j is the fraction of commodity i used by industry j to produce their output. If the volume and expenditure data are consistent, then the ratios computed from either method will be identical. For a calibrated model where the markets clear in the base year, $\sum_j \Phi_i^j = 1$ for all commodities i. We then obtain the system of equations

$$F_{j,t}\mathbf{y}_{j,t} = \sum_i \left(F_{i,t}\Phi_i^j + \bar{f}_i^j\right)\mathbf{x}_{i,t}^j \,. \tag{3}$$

Working though the simple example above and assuming the model is calibrated with $\mathbf{y}$=1 and $\mathbf{x}$=1, we obtain the equivalent system

$$\begin{aligned} F_{coal} &= 0 \\ F_{elec} &= F_{coal} + 10e_{coal} \\ F_{steel} &= 0.7F_{elec} \\ F_{auto} &= 0.3F_{elec} + F_{steel}. \end{aligned}$$

The solution to this system is

$$\begin{aligned} F_{coal} &= 0 \\ F_{elec} &= 10e_{coal} \\ F_{steel} &= 7e_{coal} \\ F_{auto} &= 10e_{coal}. \end{aligned}$$

Since consumers demand all the automobiles produced and the model is calibrated, the embedded emissions in the automobiles demanded are $F_{auto} = 10e_{coal} = 10E_{auto}$, which is consistent with the earlier calculation.

We estimate the emissions content F for each industry for given Φ, $\bar{f}$, $\mathbf{x}$, and $\mathbf{y}$ by solving the linear system of equations (3). These amounts are then used to determine the carbon taxes on imports and refunds on exports for border tax adjustments. This system has more variables than equations because of the land, labor, and capital factors. In our computations, we ignore the emissions from these factors by fixing their embedded emissions to zero. We are then left with a square system of linear equations that can be solved.

When a commodity is imported, we tax the embedded carbon emissions. In terms of quantities, the tax collected by importer j on commodity i is

$$tE_i x_i^j,$$

where t is the tax rate per unit emissions. As before, we change variables so that all quantities are measured relative to a base year. In particular,

$$tE_i x_i^j = tE_i \bar{x}_i^j \mathbf{x}_i^j = tE_i \bar{y}_i \frac{\bar{x}_i^j}{\bar{y}_i}\mathbf{x}_i^j = tF_i \frac{\bar{p}_i \bar{x}_i^j}{\bar{p}_i \bar{y}_i}\mathbf{x}_i^j = tF_i \Phi_i^j \mathbf{x}_i^j.$$

We need compute only the total emissions in each industry, F_i; the emissions per unit commodity, E_i, are not necessary.

4.2 Results for Policy Scenarios

The issue of carbon leakage has generated a significant literature and a variety of approaches to estimation have produced a wide range of leakage estimates. Babiker (2005), for example, uses the EPPA model to predict leakage in excess of 100% in one scenario based on an assumption of increasing returns to scale. There exist far fewer estimates of the effects of border tax adjustments. Babiker and Rutherford (2005) model the Kyoto Protocol and find substantial leakage and small effects from border tax adjustments.

We consider four policy scenarios in this study:

1. A reference scenario with no climate policy using the median baseline scenario described in Section 3.2 (REF).
2. A policy scenario using the median baseline scenario in which each Annex B country taxes carbon at 28.6 \$/t CO_2 (AB).
3. A policy scenario using the median baseline scenario in which each Annex B country taxes carbon and imposes a tariff on the estimated unpaid carbon content of imports from all non-Annex B countries at 28.6 \$/t CO_2 (AB-T).
4. A policy scenario using the median baseline scenario in which each Annex B country taxes carbon and assesses a border tax adjustment that taxes the estimated total carbon content of all imports and refunds the collected carbon taxes on all exports based on the total carbon content at 28.6 \$/t CO_2 (AB-BTA).

More policy scenarios can be found in Elliott et al. (2010). A carbon price of 28.6 \$/t CO_2 was chosen because it is close to the median value in proposed climate legislation. The two trade policy options AB-T and AB-BTA are examined for their effect on carbon leakage. For all policy scenarios, we solve the CGE model instance for the given year using the embedded emissions estimate from the previous year to determine the tariffs and border tax adjustments, since this approach mimics how the policies would be implemented. For the AB-T scenario where we compute only unpaid emissions content, we simply set $\bar{f}_i^j$=0 for the producers in the Annex B countries. We always use the full emissions data when computing the total emissions in the results.

To present results, we define a carbon flow matrix showing international emission flows as a result of international trade. We calculate the total emissions produced in each region from the fossil fuels burned, estimate the export emissions flows, and assign the remaining emissions to local consumption. We aggregate from 16 regions to 8 regions in the carbon flow tables for readability.

Table 4: **Fossil fuel CO_2 accounting in 2004 for the reference scenario.**

REF	Annex B					Non Annex B			
2004	USA	EUR	RUS	JAZ	CAN	CHK	LAM	ROW	Prod.
USA	5.012	0.280	0.007	0.095	0.177	0.109	0.209	0.112	6.002
EUR	0.303	3.928	0.063	0.072	0.028	0.096	0.066	0.306	4.863
RUS	0.071	0.408	1.468	0.022	0.003	0.083	0.022	0.100	2.178
JAZ	0.084	0.082	0.003	1.146	0.008	0.160	0.012	0.098	1.593
CAN	0.248	0.033	0.001	0.009	0.223	0.012	0.008	0.010	0.543
CHK	0.577	0.587	0.032	0.390	0.050	3.679	0.103	0.478	5.897
LAM	0.293	0.122	0.006	0.018	0.016	0.036	0.956	0.040	1.487
ROW	0.300	0.657	0.031	0.289	0.020	0.376	0.055	3.199	4.928
Cons.	6.888	6.096	1.610	2.043	0.5260	4.5509	1.432	4.344	27.491

Note: All numbers in billions of tonnes (Gt) CO_2. The table shows carbon producers (or exporters) on the vertical and carbon consumers (or importers) on the horizontal. The diagonal gives domestic consumption. The right column labeled "Prod." gives the total carbon produced (emitted) in each region. The bottom row labeled "Cons." gives the total carbon consumed in each region (embedded in domestic goods and imports).

The countries in each aggregate region are shown in parenthesis in the first column of Table 1. Japan and Oceania, for example, are aggregated to JAZ.

The carbon flow matrix for the reference scenario in the 2004 base year is shown in Table 4. All numbers are reported in billions of tonnes (Gt) CO_2. The row sum in the right column of the table is the total emissions generated by producers in the region, while the column sum in the bottom row shows the total embedded emissions in the commodities demanded by the consumers in each region. The difference between the row sum and the column sum determines whether the region is a net importer or exporter of emissions. In particular, USA is a net importer of 0.885 Gt CO_2, while CHK is a net exporter of 1.347 Gt CO_2. The lower-right corner indicates global emissions of 27.491 Gt CO_2. For the 2004 base year, the global emissions are in good agreement with the emissions database produced by GTAP from the IEA energy database (Lee, 2009) and with the CDIAC National Fossil-Fuel CO_2 Emissions database Boden et al. (2009). The remainder of the matrix indicates the international emission flows. The diagonal value is the emissions generated in the given region that are not exported, while the off-diagonal values are the emissions embedded in imports and exports. Looking at the USA row, of the 6.002 Gt CO_2 produced, 5.012 Gt CO_2 are embedded in commodities demanded by the USA consumer, while 0.280 Gt CO_2 are exported by USA to EUR. From the USA column, of the 6.888 Gt CO_2 in commodities demanded by the USA consumer, 5.012 Gt CO_2 were generated domestically, while 0.577 Gt CO_2 are imported by USA from CHK.

Table 5: **Percent change in emissions in 2020 for the AB policy scenario.**

AB vs. REF	Annex B USA	EUR	RUS	JAZ	CAN	Non Annex B CHK	LAM	ROW	Prod.
USA	**-27.2**	**-20.0**	-22.5	-27.0	-21.7	**-25.4**	**-30.0**	-29.6	**-26.8**
EUR	**-23.6**	**-23.3**	-19.6	-18.3	-17.7	-21.6	-23.4	**-28.2**	**-23.5**
RUS	**-38.0**	**-33.9**	**-29.4**	-34.6	-34.0	**-37.6**	-40.0	**-35.6**	**-31.5**
JAZ	-14.2	-14.4	-17.2	**-32.9**	-18.8	**-22.3**	-19.3	-25.0	**-28.8**
CAN	**-20.8**	-18.6	-16.2	-19.0	**-26.1**	-19.8	-20.1	-20.7	**-22.8**
CHK	1.1	1.8	2.0	3.0	2.0	**2.8**	2.3	1.3	**2.4**
LAM	**24.7**	14.0	47.7	4.3	25.9	3.0	**6.6**	5.4	**10.7**
ROW	8.0	**12.8**	18.5	**15.2**	8.4	**6.2**	9.6	**4.7**	**6.6**
Cons.	**-19.4**	**-15.1**	**-26.7**	**-15.6**	**-17.0**	0.3	-1.0	-0.1	**-9.9**

Note: This policy scenario has a constant 28.6 \$/t CO_2 (USD per tonne carbon) tax levied in all Annex B countries starting in 2012, relative to the reference scenario. The largest gross changes ($|\Delta E| \geq 0.05$ Gt CO_2) are shown in bold, and the smallest ($|\Delta E| \leq 0.01$ Gt CO_2) are shown faded.

Table 5 shows the carbon flow matrix for the AB policy scenario with a carbon price of 28.6 \$/t CO_2 (AB) relative to the reference scenario. The upper-left block of the matrix shows decreased trade among the Annex B regions relative to the reference scenario, while the lower-right block shows increased trade among the non-Annex B regions. The emissions embedded in exports from Annex B to non-Annex B countries shown in the upper-right block of the matrix decreases from a combination of the exporting nations switching to cleaner production processes and exporting less because the cleaner commodities are more expensive. Carbon leakage is indicated by the lower-left block of the matrix. In particular, imports to Annex B counties from non-Annex B countries increase since the commodities from non-Annex B countries are less expensive than the cleaner commodities produced domestically. As can be seen by comparing the change in total emissions produced by an Annex B region (the last column of the table) to the change in total consumed emissions (the last row in the table), the emissions from consumption for each Annex B region falls more slowly than their generation of emissions because of leakage. For example, USA reduces its generation of emissions in 2020 by 26.8% relative to the reference scenario with the AB policy, but only decreases its consumption of emissions by 19.4%. This leakage is the result of increased imports of dirty commodities from non-Annex B regions.

The addition of a tariff on embedded emissions in the AB-T policy scenario has a small, but not insubstantial effect on global emissions. Where the emissions are generated changes substantially from the AB policy scenario, as shown in Table 6. In particular, increased trade among the Annex B countries causes them to increase their emissions generated. For example, USA has a

Table 6: **Percent change in emissions in 2020 for the AB-T policy scenario.**

AB-T	Annex B					Non Annex B			
vs. REF	USA	EUR	RUS	JAZ	CAN	CHK	LAM	ROW	Prod.
USA	**-25.5**	**-18.1**	-20.7	-16.4	-19.2	**-35.8**	**-36.2**	**-37.7**	**-25.8**
EUR	-12.4	**-19.9**	-17.6	-14.9	-14.3	**-33.4**	-31.5	**-36.6**	**-21.0**
RUS	-27.8	**-30.0**	**-27.8**	-24.2	-30.9	**-49.9**	-51.6	**-45.1**	**-30.3**
JAZ	-12.8	-15.0	-17.0	**-25.8**	-18.1	**-35.5**	-28.0	-35.8	**-26.7**
CAN	-14.8	-18.6	-13.7	-16.7	**-22.3**	-32.1	-29.1	-30.7	**-19.8**
CHK	**-9.4**	**-10.5**	-12.1	**-11.1**	-11.9	**3.8**	13.6	**8.6**	**0.9**
LAM	-8.5	-4.0	10.6	-2.7	-4.6	3.6	**5.7**	7.3	**2.7**
ROW	-5.2	**-6.9**	-9.2	-8.1	-6.2	**8.0**	16.6	**4.6**	**2.8**
Cons.	**-21.1**	**-17.3**	**-26.5**	**-18.8**	**-18.6**	**0.5**	-0.8	0.2	**-10.7**

Note: A policy scenario with a constant 28.6 \$/t CO_2 (USD per tonne carbon) tax levied in all Annex B countries and on the unpaid emissions embedded in imports from non-Annex B countries starting in 2012, relative to the reference scenario.

Table 7: **Percent change in emissions in 2020 for the AB-BTA policy scenario.**

AB-BTA	Annex B					Non Annex B			
vs. REF	USA	EUR	RUS	JAZ	CAN	CHK	LAM	ROW	Prod.
USA	**-25.6**	**-19.0**	-21.4	-18.7	-20.4	**-23.9**	-16.9	-22.0	**-24.7**
EUR	-13.7	**-20.2**	-17.5	-15.9	-15.6	-25.8	-21.8	**-23.1**	**-20.1**
RUS	-31.8	**-32.6**	**-30.3**	-29.0	-33.5	-16.4	-18.9	-12.4	**-28.7**
JAZ	-13.4	-15.9	-16.5	**-26.3**	-18.8	**-25.8**	-20.4	-27.7	**-25.1**
CAN	-15.6	-19.1	-13.5	-18.2	**-23.1**	-24.7	-20.8	-22.1	**-19.6**
CHK	**-8.0**	**-8.9**	-10.0	**-9.9**	-10.3	**3.1**	9.4	**5.6**	0.3
LAM	-9.9	-2.7	15.5	-1.3	-2.8	-1.0	**4.0**	0.6	0.5
ROW	-4.1	-5.8	-6.4	-7.1	-4.5	1.8	7.9	**3.2**	**1.2**
Cons.	**-20.8**	**-17.4**	**-28.5**	**-18.4**	**-18.6**	**0.5**	0.2	0.5	**-10.8**

Note: A policy scenario with a constant 28.6 \$/t CO_2 (USD per tonne carbon) tax levied in all Annex B countries and on the total emissions embedded in all imports with refunds on all exports for the carbon taxes levied starting in 2012, relative to the reference scenario.

26.8% reduction in emissions produced in the AB scenario relative to the reference scenario, but only a 25.8% reduction in the AB-T scenario. Trade among the non-Annex B countries generally increases. However, the off-diagonal blocks show decreased trade between Annex B and non-Annex B countries, including further reductions to exports from Annex B to non-Annex B regions shown in the upper-right block of the matrix. The net result is a small reduction in global emissions. Moreover, we can see a narrowing of the change in total emissions produced by an Annex B region to the change in total consumed emissions compared to the AB policy scenario, indicating less carbon leakage.

Results from adding border tax adjustments in the Annex B countries are shown in Table 7. The refunds on the collected carbon taxes on all exports from Annex B countries results in increased production and more exports to non-Annex B countries, but reduces the amount of trade between non-Annex B countries and hence their emissions. The result is a small reduction in total global emissions. The producers in Annex B countries are better off because exports to non-Annex B countries shown in the top-right block of the matrix are reduced less under this scenario than the AB-T policy scenario. For example, USA has a 35.8% reduction in exports to CHK relative to the reference scenario under the AB-T policy scenario, but only a 23.9% reduction with the AB-BTA policy scenario. We also see a narrowing of the change in total emissions produced by an Annex B region to the change in total consumed emissions compared to the AB-T policy scenario, indicating further reductions in carbon leakage.

4.3 Results for Ensemble of Baseline Scenarios

The forecasts generated by any model instance depend on both the policy scenario and the baseline assumptions used to construct the dynamic trajectories for labor productivity and energy intensity. We now study the sensitivity of the emissions forecasts from our model to the baseline assumptions. We are most interested in gross emissions since they are used to define policy targets in international agreements and are useful for measuring carbon leakage by comparing the overall reduction in emissions from Annex B countries to subsequent increases in emissions for non-Annex B countries.

To complete this analysis, we produced forecasts of emissions with our model instance using the parameters in each of the 25 baseline scenarios outlined in Section 3.2. Figure 9 compares the reduction in USA emissions (upper plots), the reduction in total emissions from Annex B countries (middle plots), and the total increase in emissions from non-Annex B countries (lower plots) in 2020 across the range of baseline scenarios for the AB policy scenario. Each point in the figure corresponds to a set of baseline assumptions. The point in the upper left plot with coordinates $(7.87, -2.11)$ corresponds to the median baseline scenario. The first coordinate, 7.87 Gt CO_2, is the gross emissions forecast for the reference policy. The second coordinate, -2.11 Gt CO_2, indicates the change in gross emissions for the AB policy scenario relative to the reference policy with the same baseline. The sum of the two coordinates, 5.76, is the gross emissions forecast for the AB policy scenario with the median

Figure 9: **Policy implications of AB scenario.**

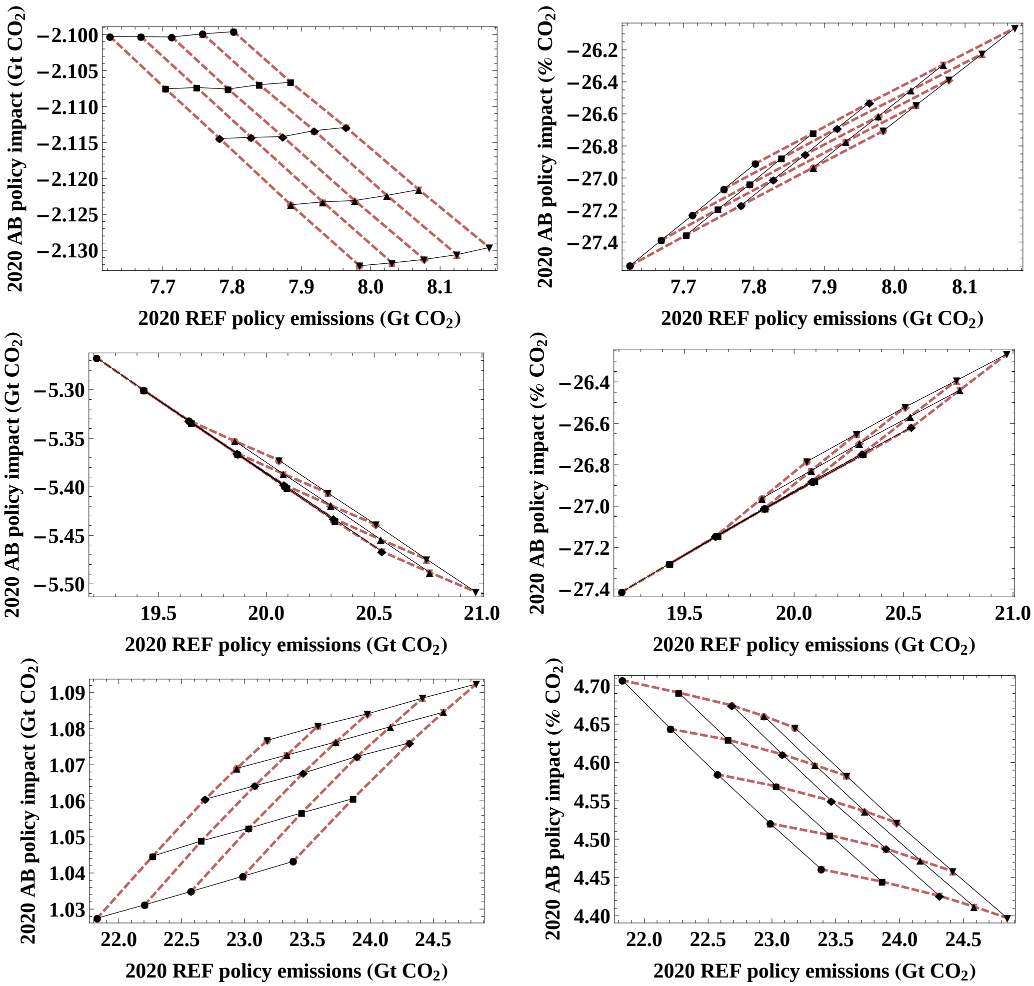

Note: Each point in the plots corresponds to a baseline scenario. The coordinates are the forecasts for the reference policy and the AB policy scenario. Along the horizontal, each baseline scenario is ranked by the gross CO_2 emissions in 2020 for the reference policy. On the vertical, we plot the impact of the AB policy scenario. The left plots measures gross emissions reductions, while the right plots measures percent reductions. The upper, middle, and lower plots are for the USA, Annex B counties, and non-Annex B countries, respectively. Points connected by solid black lines have a fixed value of the labor productivity parameter and varying energy intensity; points connected by red dashed lines have fix energy intensity.

baseline scenario. The right plots are similar except the second coordinate is the percent change in emissions relative to the reference policy.

The points are connected with solid black lines to indicate baseline scenarios with the same value of the labor productivity parameter and varying energy intensity. The points connected with red dashed lines have the same value of the energy intensity parameter and varying labor productivity. The top black line in the upper-left plot corresponds to baseline scenarios with the minimum value for the rate of change in labor productivity, while the bottom black line is the baseline scenarios with the maximum value. The left dashed line is the scenarios with the lowest rate of change in energy intensity, while the right dashed line is the highest. The slope of the lines indicates the sensitivity of the metric to different rates of change in energy intensity (black lines) or labor productivity (red dashed lines). Flat lines, such as the black lines found in the upper-left plot of the gross reduction in emissions for the AB policy scenario relative to the reference policy for the USA, indicate low sensitivity, while more vertical lines indicate higher sensitivity.

The relative impact of the policy on gross emissions in the Annex B countries appears to be more sensitive to the rate of change in energy intensity than to the rate of change in labor productivity. The USA is a notable exception, where gross emissions reductions are more sensitive to the rate of change in labor productivity than to the rate of change in energy intensity. Measured in percent reduction relative to the reference policy, the ensemble of baseline scenarios has a sensitivity range for gross emissions in the Annex B countries of about 1.3%. Emissions increases in the non-Annex B regions are more sensitive to changes in labor productivity than to energy intensity.

Overall, the median baseline scenario shows a decrease of 5.4 Gt CO_2 across the Annex B counties and an increase in emissions of 1.07 Gt CO_2 across the non-Annex B countries, implying almost 20% carbon leakage. Unsurprisingly, baseline scenarios with higher emissions lead to more carbon leakage, since Annex B regions are forced to pay more carbon taxes for production. In percent terms, the carbon leakage is less sensitive to different rates of change in labor productivity than to different rates of change in energy intensity.

In the USA, the ensemble of baseline scenarios shows a gross 2020 emissions range of 7.6–8.1 Gt CO_2 or about 6% of the median value, with a gross emissions reduction range of 2.10–2.13 Gt CO_2 or about 1.5% of the median value. In aggregate, the range across all Annex B countries is almost 10% of median gross emissions and the gross emissions reduction is around 4.5% of the median value. The results across the non-Annex B countries are similar with a range of almost 13% of the median value for gross emissions and a range of about 5.5% of the median value for gross emissions reductions. Given that these results are over a fairly compact ensemble of baseline scenarios when compared to the span of the EIA baseline forecasts over the past five years shown in Figure 6, measuring policy impacts with high accuracy against historical targets, such as the USA emissions target under the nonbinding international agreement from the December 2009 Copenhagen meeting of a 17% reduction from 2005 emissions levels by 2020, would be difficult.

5 Conclusion

In this paper, we introduced the CIM-EARTH framework for specifying CGE models, detailed a model instance used to study the impact of carbon emission policies, and presented results for a handful of policies and the sensitivity of those results to baseline assumptions on the rate of change in both the labor productivity and energy intensity trajectories. Additionally, we described a method for measuring embedded carbon in commodities, used it to estimate carbon content in international trade flows, and introduced a matrix method to display international emissions flows to highlight the major mitigation impacts of climate policies.

Many extensions to the modeling framework are either under development or planned. In particular, we are planning to introduce fully dynamic CGE models and to augment the set of building blocks available to assemble model instances. These building blocks include capital and product vintages (Benhabib and Rustichini, 1991; Cadiou et al., 2003; Salo and Tahvonen, 2003) and overlapping consumer generations (Auerbach and Kotlikoff, 1987). We also plan to add private learning, research and development, and technology adoption (Boucekkine and Pommeret, 2004; Futagami and Iwaisako, 2007; Hritonenko, 2008; Zou, 2006) and to include household production functions, nonseparable utility functions, and heterogeneous beliefs.

Our framework allows us to systematically explore the sensitivity of the simulation results to a wide range of input uncertainties including the elasticities of substitution, the base-year expenditure and revenue data, and the assumptions used to construct the dynamic trajectories. To explore the sensitivity of policy-relevant metrics to the dynamic trajectories, we constructed an ensemble of baseline scenarios. Our results indicate that the gross reduction in emissions relative to the reference policy is more sensitive to energy intensity than to labor productivity across the Annex B countries. The exception is the USA, which is much more sensitive to labor productivity than to energy efficiency. The non-Annex B countries are more sensitive to labor productivity. Given the range of results across our relatively small ensemble of baseline scenarios, measuring policy impacts against historical targets, such as a 17%

emissions reduction from 2005 levels by 2020 in the USA, with high accuracy may already be problematic.

References

Auerbach, A. J. and L. J. Kotlikoff (1987): *Dynamic Fiscal Policy*, Cambridge, U.K.: Cambridge University Press.

Babiker, M. H. (2005): "Climate Change Policy, Market Structure, and Carbon Leakage," *Journal of International Economics*, 65, 421–445.

Babiker, M. H., J. Reilly, M. Mayer, R. S. Eckaus, I. S. Wing, and R. C. Hyman (2001): "The MIT Emissions Prediction and Policy Analysis (EPPA) Model: Revisions, Sensitivities, and Comparisons of Results," Technical Report 71, MIT Joint Program Report Series, URL `http://globalchange.mit.edu/pubs/abstract.php?publication_id=643`.

Babiker, M. H. and T. F. Rutherford (2005): "The Economic Effects of Border Measures in Subglobal Climate Agreements," *The Energy Journal*, 26, 99–126.

Balay, S., W. D. Gropp, L. C. McInnes, and B. F. Smith (1997): "Efficient Management of Parallelism in Object Oriented Numerical Software Libraries," in E. Arge, A. M. Bruaset, and H. P. Langtangen, eds., *Modern Software Tools in Scientific Computing*, Birkhauser Press, 163–202.

Balistreri, E. J., C. A. McDaniel, and E. V. Wong (2003): "An Estimation of U.S. Industry-Level Capital-Labor Substitution," Computational Economics 0303001, EconWPA, URL `http://ideas.repec.org/p/wpa/wuwpco/0303001.html`.

Ballard, C., D. Fullerton, J. B. Shoven, and J. Whalley (1985): *A General Equilibrium Model for Tax Policy Evaluation*, National Bureau of Economic Research Monograph, University of Chicago Press.

Benhabib, J. and A. Rustichini (1991): "Vintage Capital, Investment, and Growth," *Journal of Economic Theory*, 55, 323–339.

Benson, S., L. C. McInnes, J. Moré, T. Munson, and J. Sarich (2010): *Toolkit for Advanced Optimization (TAO) Web Page*, URL `http://www.mcs.anl.gov/tao`.

Bhattacharyya, S. C. (1996): "Applied General Equilibrium Models for Energy Studies: A Survey," *Energy Economics*, 18, 145–164.

Boden, T., G. Marland, and R. Andres (2009): *Global, Regional, and National Fossil-Fuel CO_2 Emissions*, Carbon Dioxide Information Analysis Center, Oak Ridge National Laboratory, U.S. Department of Energy, Oak

Ridge, Tenn. U.S.A., URL http://cdiac.ornl.gov/trends/emis/tre_glob.html, doi 10.3334/CDIAC/00001_V2010.

Boehringer, C., T. F. Rutherford, and W. Wiegard (2003): "Computable General Equilibrium Analysis: Opening a Black Box," Discussion Paper 03-56, ZEW, URL ftp://ftp.zew.de/pub/zew-docs/dp/dp0356.pdf.

Boucekkine, R. and A. Pommeret (2004): "Energy Saving Technical Progress and Optimal Capital Stock: The Role of Embodiment," *Economic Modelling*, 21, 429–444.

Burniaux, J.-M. and T. Truong (2002): "GTAP-E: An Energy-Environmental Version of the GTAP Model," GTAP Technical Papers 923, Center for Global Trade Analysis, Department of Agricultural Economics, Purdue University, URL http://ideas.repec.org/p/gta/techpp/923.html.

Cadiou, L., S. Dées, and J.-P. Laffargue (2003): "A Computational General Equilibrium Model with Vintage Capital," *Journal of Economic Dynamics and Control*, 27, 1961–1991.

Conrad, K. (2001): "Computable General equilibrium Models in Environmental and Resource Economics," IVS discussion paper series 601, Institut für Volkswirtschaft und Statistik, University of Mannheim, URL http://ideas.repec.org/p/mea/ivswpa/601.html.

Davis, S. J. and K. Caldeira (2010): "Consumption-based Accounting of CO_2 Emissions," *Proceedings of the National Academy of Sciences*, doi 10.1073/pnas.0906974107.

de la Chesnaye, F. C. and J. P. Weyant, eds. (2006): *Multi-Greenhouse Gas Mitigation and Climate Policy*, The Energy Journal, Special Issue.

de Melo, J. (1988): "CGE Models for the Analysis of Trade Policy in Developing Countries," Policy Research Working Paper Series 3, The World Bank, URL http://ideas.repec.org/p/wbk/wbrwps/3.html.

del Negro, M. and F. Schorfheide (2003): "Take Your Model Bowling: Forecasting with General Equilibrium Models," *Economic Review*, 35–50.

Devarajan, S. and S. Robinson (2002): "The Influence of Computable General Equilibrium Models on Policy," TMD discussion papers 98, International Food Policy Research Institute (IFPRI), URL http://ideas.repec.org/p/fpr/tmddps/98.html.

Dirkse, S. P. and M. C. Ferris (1995): "The PATH Solver: A Non-Monotone Stabilization Scheme for Mixed Complementarity Problems," *Optimization Methods and Software*, 5, 123–156.

Dowlatabadi, H. and M. G. Morgan (1993): "Integrated Assessment of Climate Change," *Science*, 259, 1813–1932.

Elliott, J., I. Foster, S. Kortum, T. Munson, F. Pérez Cervantes, and D. Weisbach (2010): "Trade and Carbon Taxes," *American Economic Review: Pa-*

pers and Proceedings, 100, 465–469.

Ferris, M. C. and T. Munson (1999): "Interfaces to PATH 3.0: Design, Implementation and Usage," *Computational Optimization and Applications*, 12, 207–227.

Ferris, M. C. and T. Munson (2001): *GAMS/PATH User Guide: Version 4.6*, Department of Computer Sciences, University of Wisconsin, Madison, URL `ftp://ftp.cs.wisc.edu/math-prog/solvers/path/pathlib/doc/gams_user.ps`.

Fourer, R., D. M. Gay, and B. W. Kernighan (2003): *AMPL: A Modeling Language for Mathematical Programming*, Pacific Grove, California: Brooks/Cole–Thomson Learning, second edition.

Fullerton, D., ed. (2009): *Distributional Effects of Environmental and Energy Policy*, Surrey, U.K.: Ashgate Publishing.

Fullerton, D. and D. L. Rogers (1993): *Who Bears the Lifetime Tax Burden?*, Washington, D.C.: Brookings Institution Press.

Futagami, K. and T. Iwaisako (2007): "Dynamic Analysis of Patent Policy in an Endogenous Growth Model," *Journal of Economic Theory*, 132, 306–334.

Ginsburgh, V. and M. Keyzer (1997): *The Structure of Applied General Equilibrium Models*, Cambridge, MA: The MIT Press.

Gopalakrishnan, B. N. and T. L. Walmsley, eds. (2008): *Global Trade, Assistance, and Production: The GTAP 7 Data Base*, Purdue University: Global Trade Analysis Center, Department of Agricultural Economics, URL `https://www.gtap.agecon.purdue.edu/databases/v7/v7_doco.asp`.

Hritonenko, N. (2008): "Modeling of Optimal Investment in Science and Technology," *Nonlinear Analysis: Hybrid Systems*, 2, 220–230.

International Labor Organization (2009): *Key Indicators of the Labour Market*, International Labour Organization Economic and Labour Market Analysis Department, URL `http://www.ilo.org/empelm/`.

International Labor Organization (2010): *Yearbook of Labour Statistics Database*, International Labor Organization Department of Statistics, URL `http://laborsta.ilo.org`.

Johansen, L. (1960): *A Multisectoral Study of Economic Growth*, Amsterdam: North Holland.

Lee, H.-L. (2009): *An Emissions Data Base for Integrated Assessment of Climate Change Policy Using GTAP*, URL `https://www.gtap.agecon.purdue.edu/resources/download/4470.pdf`.

Lee, N. (2006): "Bridging the Gap Between Theory and Practice in Integrated Assessment," *Environmental Impact Assessment Review*, 26, 57–78.

Liu, J., C. Arndt, and T. Hertel (2004): "Parameter Estimation and Measures of Fit in A Global, General Equilibrium Model," *Journal of Economic*

Integration, 19, 626–649.

Nakicenovic, N., J. Alcamo, G. Davis, B. de Vries, J. Fenhann, S. Gaffin, K. Gregory, A. Grübler, T. Jung, and T. K. et al. (2000): *Intergovernmental Panel on Climate Change Special Report on Emissions Scenarios*, Cambridge, U.K.: Cambridge University Press.

Robinson, S. (1991): "Macroeconomics, Financial Variables, and Computable General Equilibrium Models," *World Development*, 19, 1509–1525.

Salo, S. and O. Tahvonen (2003): "On the Economics of Forest Vintages," *Journal of Economic Dynamics and Control*, 27, 1411–1435.

Scarf, H. E. and J. B. Shoven (1984): *Applied General Equilibrium Analysis*, Cambridge, U.K.: Cambridge University Press.

Scrieciu, S. S. (2007): "The Inherent Dangers of Using Computable General Equilibrium Models as a Single Integrated Modelling Framework for Sustainability Impact Assessment: A Critical Note on Bohringer and Loschel (2006)," *Ecological Economics*, 60, 678–684.

Shoven, J. B. and J. Whalley (1984): "Applied General-Equilibrium Models of Taxation and International Trade: An Introduction and Survey," *Journal of Economic Literature*, 22, 1007–1051.

Sokolov, A. P., P. H. Stone, C. E. Forest, R. Prinn, M. C. Sarofim, M. Webster, S. Paltsev, C. A. Schlosser, D. Kicklighter, S. Dutkiewicz, J. Reilly, C. Wang, B. Felzer, J. M. Melillo, and H. D. Jacoby (2009): "Probabilistic Forecast for Twenty-First-Century Climate Based on Uncertainties in Emissions (Without Policy) and Climate Parameters," *Journal of Climate*, 22, 5175–5204.

Sue Wing, I. (2004): "Computable General Equilibrium Models and Their Use in Economy-Wide Policy Analysis," Technical Note 6, Joint Program on the Science and Policy of Global Change, URL `http://globalchange.mit.edu/files/document/MITJPSPGC_TechNote6.pdf`.

United Nations (2008): *World Population Prospects: The 2008 Revision Population Database*, United Nations Population Division, URL `http://esa.un.org/unpp`.

United States Energy Information Agency (2009): *International Energy Outlook*, United States Energy Information Agency, report DOE/EIA-0484, URL `http://www.eia.doe.gov/`.

Vuuren, D., J. Lowe, E. Stehfest, L. Gohar, A. Hof, C. Hope, R. Warren, M. Meinshausen, and G.-K. Plattner (2009): "How Well do IAMs Model Climate Change?" *IOP Conference Series: Earth and Environmental Science*, 6, 2005.

Webster, M., S. Paltsev, J. Parsons, J. Reilly, and H. Jacoby (2008): "Uncertainty in Greenhouse Emissions and Costs of Atmospheric Stabilization," Technical Report 165, MIT Joint Program Report Series, URL `http://globalchange.mit.edu/files/document/MITJPSPGC_Rpt165.pdf`.

Weyant, J. (2009): "A Perspective on Integrated Assessment," *Climatic Change*, 95, 317–323.

Weyant, J. P. (1999): *Energy and Environmental Policy Modeling*, Boston, MA: Kluwer Academic.

Zou, B. (2006): "Vintage Technology, Optimal Investment, and Technology Adoption," *Economic Modeling*, 23, 515–533.